Polyaniline/TiO_2 Composite Nanotubes

Lijuan Zhang and Meixiang Wan*

Organic Solid Laboratory, Center for Molecular Sciences, Institute of Chemistry, Chinese Academy of Sciences, Beijing 100080, China

Received: January 17, 2003; In Final Form: April 12, 2003

Polyaniline (PANI) composite nanotubes (90−130 nm in diameter) containing titanium dioxide (TiO_2) nanoparticles (about 10 nm in diameter) were synthesized through a self-assembly process in the presence of β-naphthalenesulfonic acid (β-NSA) as the dopant. It was found that the morphology, size, conductivity, and hydrophobicity of the PANI−β-NSA/TiO_2 composite nanotubes were affected by the content of TiO_2 nanoparticles in the nanotubes. The micelles composed of β-NSA anions and anilinium cations containing TiO_2 were proposed to interpret the formation mechanism of the self-assembled composite nanotubes. The Raman spectra and X-ray diffraction characterizations show that the main chain of the composite nanotubes is identical to that of the doped PANI, and indicate that there is no chemical interaction between PANI and TiO_2.

Introduction

Conducting polyaniline (PANI) is one of the promising conducting polymers due to its high conductivity, ease of preparation, good environmental stability, and large variety of applications such as in electrochromic devices, light-emitting diodes, chromatography, secondary batteries, electrostatic discharge protection, and corrosion-protecting paint.[1] Nowadays, one-dimensional conducting polymer nanostructures, including nanotubes or nanowires, have received great attention because of their unique properties and promising potential applications in electrical nanodevices.[2−4] One-dimensional PANI nanostructures have been synthesized both chemically and electrochemically through polymerization of the monomer with the aid of either an external template (e.g., anodized alumina or track-etched polycarbonate)[5,6] or a self-assembly process.[7−9] In addition, the multifunctionalized PANI nanotubes or nanowires have also been synthesized either by doping with a functional dopant[10,11] or by blending with inorganic electrical, optic, and magnetic nanoparticles to form composite nanostructures.[12]

Among those inorganic nanoparticles, titanium dioxide (TiO_2) nanoparticles have received great attention because of their unique electrical and optic properties as well as extensive application in diverse areas.[13−17] Although many papers on PANI/TiO_2 composites have been published in the literature,[18−22] no paper dealing with PANI/TiO_2 composite nanotubes has been published yet.

We have successfully synthesized PANI composite nanotubes with an average diameter of 90−130 nm through a self-assembly process in the presence of β- naphthalenesulfonic acid (β-NSA) as a dopant. Herein, we report the influence of the TiO_2 concentration on the morphology, size, molecular structure, electrical properties, and hydrophobicity of the PANI−β-NSA/TiO_2 composite nanotubes. The formation mechanism of the composite nanotubes is also discussed.

Experimental Section

Aniline, β-NSA, and ammonium persulfate ($(NH_4)_2S_2O_8$, APS) were purchased from Beijing Chemical Reagent Co. Aniline was distilled under reduced pressure. β-NSA as the dopant and APS as the oxidant were used as received without further treatment. TiO_2 nanoparticles (10 nm in diameter) were also used as received.

The PANI−β-NSA/TiO_2 nanotubes were synthesized by in situ doping polymerization in the presence of TiO_2 nanoparticles and β-NSA as the dopant without an external template. This method belongs to the self-assembly process because of the dopant acting with doping and template functions at the same time. A typical preparation process for PANI−β-NSA/TiO_2 nanotubes is as follows: TiO_2 was added to a 5 mL aqueous solution of β-NSA (1×10^{-3} molar) under ultrasonication for 1 h to obtain a uniform suspension containing TiO_2 nanoparticles. Aniline (2×10^{-3} M) was mixed with 5 mL of distilled water under ultrasonication for 30 min and then added to the above suspension to form an aniline/β-NSA mixture containing TiO_2. The mixture was cooled in an ice bath for 2 h before oxidative polymerization. Finally, 5 mL of a precooled aqueous solution of APS (2×10^{-3} M) was added to the above cooled mixture, and the resulting mixture was allowed to react in the ice bath for 18 h. The precipitated powder was filtered and washed with distilled water and methanol till the filtrate became colorless and then dried in a vacuum at room temperature for 24 h. Throughout the experiment, the molar ratio of aniline to β-NSA (represented by [An]:[β-NSA]) and to APS (represented by [An]:[APS]) for either PANI−β-NSA nanotubes or PANI−β-NSA/TiO_2 composite nanotubes was retained at 1:0.5 and 1:1, respectively. But the concentration of TiO_2 nanoparticles was changed to understand the effect of the TiO_2 nanoparticles on the morphology, structure, electrical properties, and hydrophobicity of the resulting PANI−β-NSA/TiO_2 composite nanotubes.

The morphologies of the PANI−β-NSA nanotubes and its composite nanotubes were examined by a JEOL JSM-6700F field emission scanning electron microscope and a JEOL JEM-2010F transmission electron microscope, respectively. The samples for scanning electron microscopy (SEM) were mounted on aluminum studs using adhesive graphite tape and sputter-coated with gold before analysis, and for transmission electron microscopy (TEM) measurements, they were dispersed on

* To whom correspondence should be addressed. E-mail: wanmx@iccas.ac.cn.

10.1021/jp034130g CCC: $25.00
Published on Web 06/20/2003

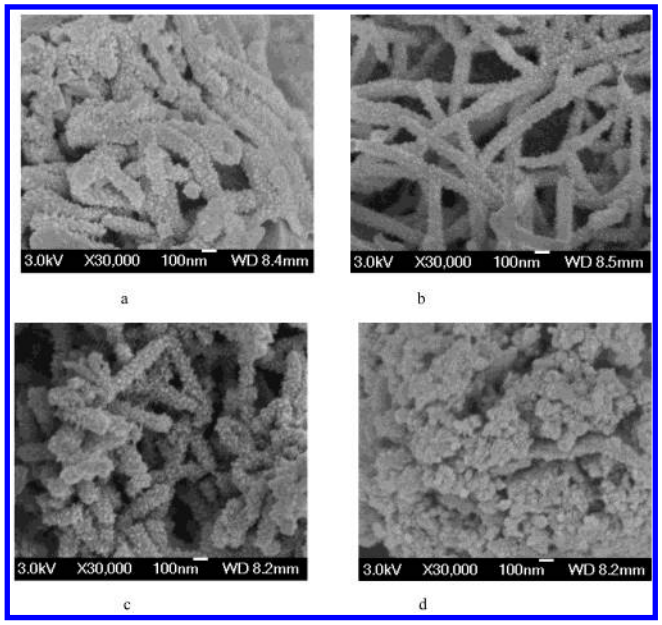

Figure 1. SEM images of PANI−β-NSA/TiO_2 synthesized under different concentrations of TiO_2: (a) 0 M, (b) 0.04 M, (c) 0.08 M, (d) 0.12 M. Synthetic conditions: [An] = 0.4 M, [An]:[β-NSA] = 1:0.5, [An]:[APS] = 1:1, reaction time 18 h, reaction temperature 0 °C.

copper microgrids coated with a carbon support film. When the TEM was investigated, the synchronous energy-dispersive X-ray analysis was recorded with a LINK ISIS300 instrument. Raman spectra of PANI−β-NSA/TiO_2 and PANI−β-NSA were carried out on a Renishaw microscope (RM-2000) with a 633 nm laser as the excitation light. The X-ray scattering patterns of PANI−β-NSA/TiO_2 and PANI−β-NSA were recorded on an X-ray diffraction instrument (Micscience M-18XHF with Cu Kα radiation). The electrical conductivity of compressed pellets at room temperature was measured by a standard four-probe method using a Keithley 196 System DMM digital multimeter and an Advantest R1642 programmable dc voltage/current generator as the current source. The temperature dependence of the conductivity for the PANI−β-NSA and PANI−β-NSA/TiO_2 pellets from 300 to 77 K was measured by a four-probe method using a Keithley 220 programmable current source and 181 nanovoltmeter. The water contact angle of PANI−β-NSA/TiO_2 and PANI−β-NSA films deposited on the glass substrate was measured by a contact angle system, OCA Data Physics DCAT 11.

Results and Discussion

1. Morphology and Its Formation Mechanism. It was found that the TiO_2 concentration strongly affected the morphology of the resulting PANI−β-NSA/TiO_2 composites as shown in Figure 1. As one can see, when the concentration of TiO_2 was lower than 0.08 M, PANI−β-NSA/TiO_2 was fibers (see Figure 1a−c); however, granular PANI−β-NSA/TiO_2 was observed when the concentration of TiO_2 was 0.12 M (Figure 1d). TEM images proved that those fibers were hollow, but sometimes solid fibers can also be seen (Figure 2). Moreover, the diameter of PANI−β-NSA/TiO_2 nanotubes was also related to the concentration of TiO_2 as shown in Figure 3. It shows that when the concentration of TiO_2 is in the range of 0.04−0.06 M, a minimum diameter (about 95 nm) for PANI−β-NSA/TiO_2 is observed. Synchronous energy-dispersive X-ray spectrum measurements revealed that the titanium element is clearly seen to be in the wall of the composite nanotubes as shown in Figure 4a, which, however, is absent in the PANI−β-NSA nanotubes

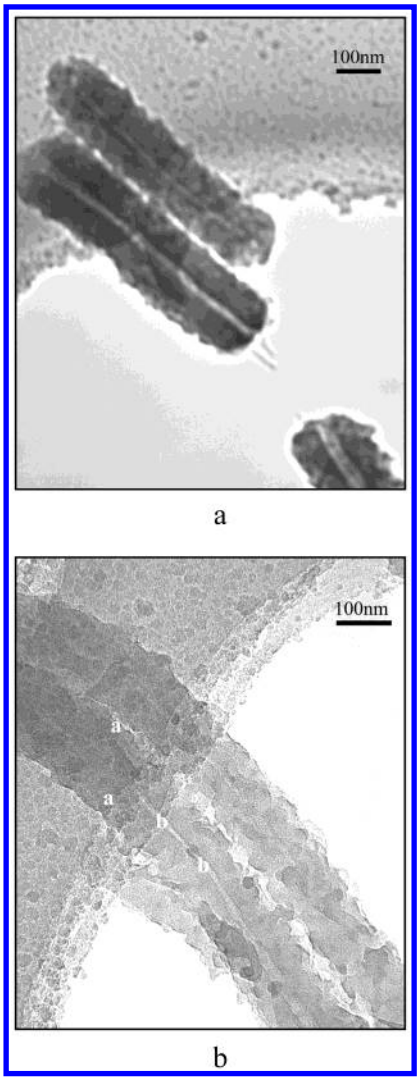

Figure 2. TEM images of PANI−β-NSA (a) and PANI−β-NSA/TiO_2 (b) nanorods or nanotubes. Synthetic conditions: [An] = 0.4 M, [An]:[β-NSA] = 1:0.5, [An]:[APS] = 1:1, reaction time 18 h, reaction temperature 0 °C, (a) without TiO_2, (b) [TiO_2] = 0.4 M.

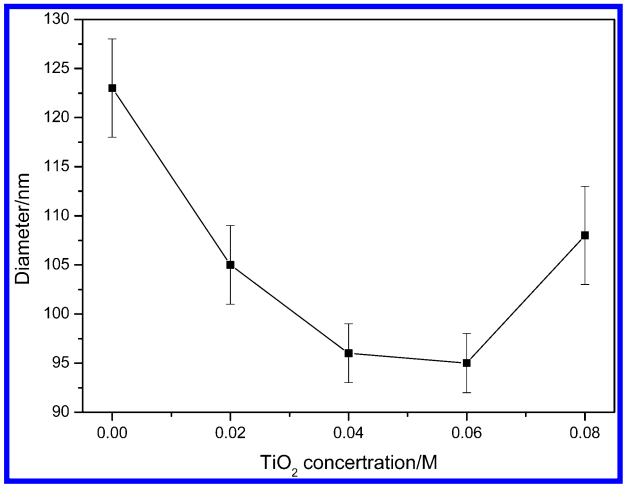

Figure 3. Influence of the TiO_2 concentration on the diameter of PANI−β-NSA/TiO_2 nanotubes. Synthetic conditions: [An] = 0.4 M, [An]:[β-NSA] = 1:0.5, [An]:[APS] = 1:1, reaction time 18 h, reaction temperature 0 °C.

(Figure 4b). This further suggested that PANI and TiO_2 nanoparticles costructured to form the composite nanotubes through a self-assembly process that is quite different from that

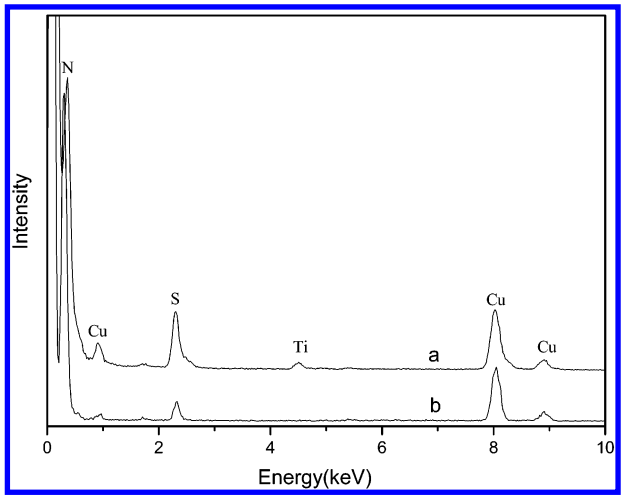

Figure 4. Energy-dispersive X-ray data from (a) the wall of and (b) inside PANI−β-NSA/TiO_2 nanotubes. Synthetic conditions: [An] = 0.4 M, [An]:[β-NSA] = 1:0.5, [An]:[APS] = 1:1, reaction time 18 h, reaction temperature 0 °C, [TiO_2] = 0.04 M.

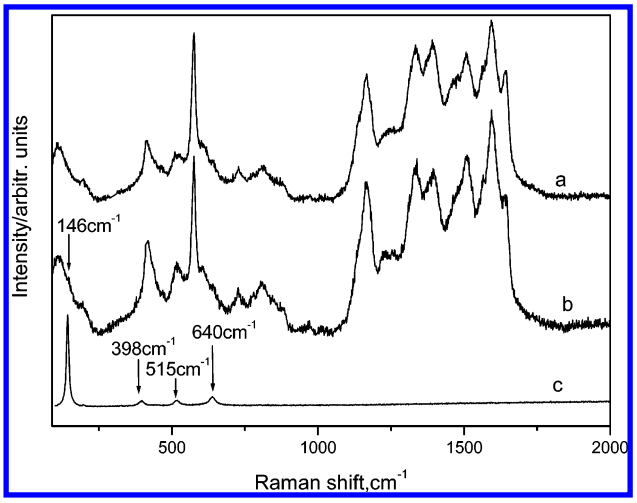

Figure 5. Raman spectra of PANI−β-NSA (a), PANI−β-NSA/TiO_2 (b), and TiO_2 nanoparticles (c), excited with a λ_L = 632.8 nm laser line. Synthetic conditions: [An] = 0.4 M, [An]:[β-NSA] = 1:0.5, [An]:[APS] = 1:1, reaction time 18 h, reaction temperature 0 °C, (a) without TiO_2, (b) [TiO_2] = 0.04 M.

of coated carbon nanotubes (CNTs) with a conducting polymer[23] or filled CNTs with other inorganic particles.[24]

On the basis of our previous studies,[25−29] the micelles formed by β-NSA anions and anilinium cations might act as templates in the formation of the self-assembled PANI nanotubes of conducting polymers. Generally speaking, β-NSA easily forms micelles in aqueous solution due to its hydrophobic (naphthalene ring) and hydrophilic ($-SO_3H$) groups. As described in the experiment, TiO_2 nanoparticles were dispersed in β-NSA aqueous solution before polymerization. As a result, it is reasonable to believe that the micelles containing TiO_2 nanoparticles might form in the reaction system. Those micelles have a "core−shell" structure, where TiO_2 nanoparticles are assigned as the "core" of the micelles due to their hydrophobic feature, while β-NSA is regarded as the "shell" of the micelles due to its hydrophilic $-SO_3H$ group. In addition, aniline reacts with β-NSA to form an aniline/β-NSA salt via an acid/base reaction. Thus, the formed anilinium cations might be absorbed on the surface of those core−shell micelles to form spherical micelles by aggregation. At the same time, free aniline existing in the reaction solution might diffuse into those micelles to form aniline-filled micelles. Thus, those micelles containing TiO_2 with or without free aniline act as templates in the formation of PANI−β-NSA/TiO_2 nanofibers or nanotubes, respectively. Since APS is water soluble, the polymerization only took place at the micelle/water interface.[30] With the polymerization proceeding, the micelles containing TiO_2 would become bigger spheres by accretion[31] or tubes/fibers by elongation,[32,33] depending on the local reaction environment. The above proposal suggests that the PANI and TiO_2 nanoparticles costructure to form composite nanotubes through a self-assembly process. If this were the case, the titanium element would be detected in the wall of the composite nanotubes. Synchronous energy-dispersive X-ray spectrum measurements proved that the TiO_2 nanoparticles are embedded in the wall of the composite nanotubes as shown in Figure 4a. Moreover, the proposal predicates that the micelles with or without free aniline, which are acting as templates in the formation of the composite nanotubes or nanofibers, respectively, coexist in the reaction. This is consistent with what we have observed in Figure 1. On the basis of the proposal, it is accepted that the formation and size of the micelles acting as templates are related to the concentration of TiO_2 nanoparticles in the reaction, resulting in the formation yield and size of the composite nanotubes being affected by the concentration of TiO_2 nanoparticles.

2. Structural Characterization. The Raman spectra of PANI−β-NSA/TiO_2, PANI−β-NSA, and TiO_2 nanoparticles are shown in Figure 5. All characteristic bands of PANI in both PANI−β-NSA (Figure 5a) and PANI−β-NSA/TiO_2 (Figure 5b) nanotubes were observed. For instance, bands at 1161 cm^{-1} corresponding to the C−H bending vibration of the benzenoid or quinoid rings,[34] 1506 cm^{-1} attributed to the N−H stretching mode, 1594 cm^{-1} assigned to the C−C stretching vibration of the benzenoid, and 1396 cm^{-1} related to the C−C stretching vibration of the quinoid rings[35−37] were observed. Other bands centered at 812 and 411 cm^{-1} are related to the C−H deformation. The band at 572 cm^{-1} is attributed to the amine deformation, and the band at 514 cm^{-1} is ascribed to the C−N−C torsion.[37] In addition, a band at 1336 cm^{-1} ascribed to the $C-N^{\bullet+}$ stretching vibration[36,37] was also observed, indicating that the PANI−β-NSA/TiO_2 and PANI nanotubes were in the doping state.

The Raman spectrum of TiO_2 nanoparticles showed four characteristic modes at 146, 398, 515, and 640 cm^{-1} (Figure 5c). The mode at 146 cm^{-1} is strong and assigned as the E_g phonon of the anatase structure and B_{1g} phonon of the rutile structure, which can also be observed in the Raman spectrum of PANI−β-NSA/TiO_2 composite nanotubes (Figure 5b). The latter three modes are assigned as B_{1g}, A_{1g}, and E_g modes of the anatase phase,[38,39] respectively. These modes of TiO_2 nanoparticles are weak and coincide with the characteristic bands of PANI−β-NSA at 412, 514, and 642 cm^{-1}, respectively.

Figure 6 shows the X-ray diffraction patterns of PANI−β-NSA/TiO_2, PANI−β-NSA, and TiO_2 nanoparticles. It was found that TiO_2 nanoparticles are crystalline (Figure 6c), and the positions of all the sharp peaks are in good agreement with the results reported by Tang et al.[40] On the other hand, PANI−β-NSA nanotubes are amorphous; only two broad peaks centered at $2\theta = 21°$ and 25° were observed (Figure 6a), which are ascribed to the periodicity parallel and perpendicular to the polymer chain,[41] respectively. However, the X-ray scattering pattern of PANI−β-NSA/TiO_2 composite nanotubes has not only one broad peak at $2\theta = 21°$ corresponding to PANI−β-NSA, but also all the sharp peaks of TiO_2 nanoparticles, proving the existence of TiO_2 nanoparticles in the composite nanotubes.

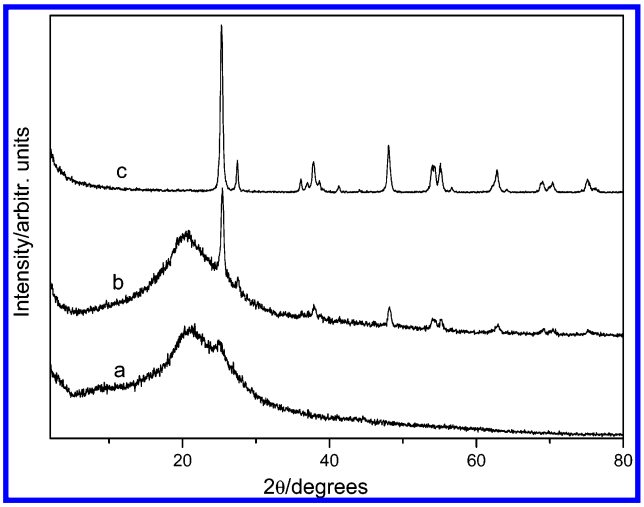

Figure 6. X-ray scattering patterns of PANI−β-NSA (a), PANI−β-NSA/TiO_2 (b), and TiO_2 nanoparticles (c), excited with a $\lambda_L = 633$ nm laser line. Synthetic conditions: [An] = 0.4 M, [An]:[β-NSA] = 1:0.5, [An]:[APS] = 1:1, reaction time 18 h, reaction temperature 0 °C, (a) without TiO_2, (b) [TiO_2] = 0.04 M.

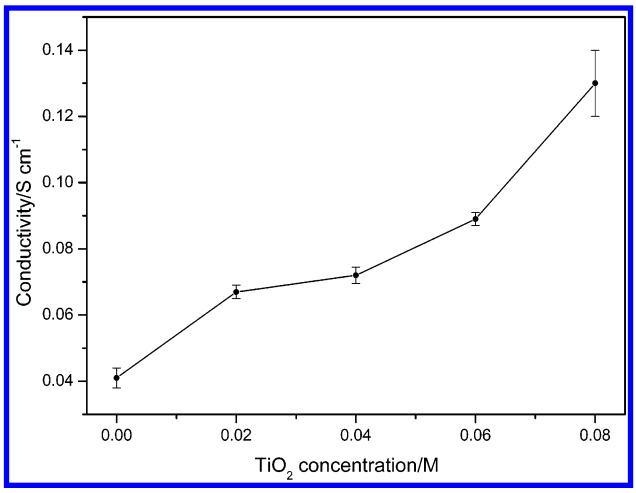

Figure 7. Effect of the TiO_2 concentration on the room-temperature conductivity of PANI−β-NSA/TiO_2 nanotubes. Synthetic conditions: [An] = 0.4 M, [An]:[β-NSA] = 1:0.5, [An]:[APS] = 1:1, reaction time 18 h, reaction temperature 0 °C.

As described above, thus, there is no chemical interaction between PANI and TiO_2 nanoparticles in the PANI−β-NSA/TiO_2 nanotubes.

3. Electrical Properties and Hydrophobicity. It was found that the conductivity of PANI−β-NSA/TiO_2 nanotubes strongly depends on their morphologies associated with the alignment effect. For instance, the conductivity of granular PANI−β-NSA/TiO_2 synthesized at a TiO_2 concentration of 0.12 M is dropped 2 orders of magnitude (reduced from 1.2×10^{-1} to 4.4×10^{-3} S/cm) compared with that of tubular PANI−β-NSA/TiO_2. This indicates that higher conductivity observed from the nanotubes may be caused by their tubular morphologies, which might result in some alignment of the polymer chain along the nanotubes. In particular, the conductivity of the PANI−β-NSA/TiO_2 nanotubes increases with an increase of the TiO_2 concentration as shown in Figure 7. This is consistent with the results of PANI−DBSA/TiO_2 reported by Su et al.[20] In our case, however, the size effect of the PANI−β-NSA/TiO_2 nanotubes on their conductivity might need to be considered because the diameter of the PANI−β-NSA/TiO_2 nanotubes was reduced with an increase of the TiO_2 concentration (Figure 3). This agrees with the results reported by Martin et al.[42] The above results also indicate that changing the TiO_2 concentration in the composites can control the conductivity and the diameter of the PANI−β-NSA/TiO_2 nanotubes.

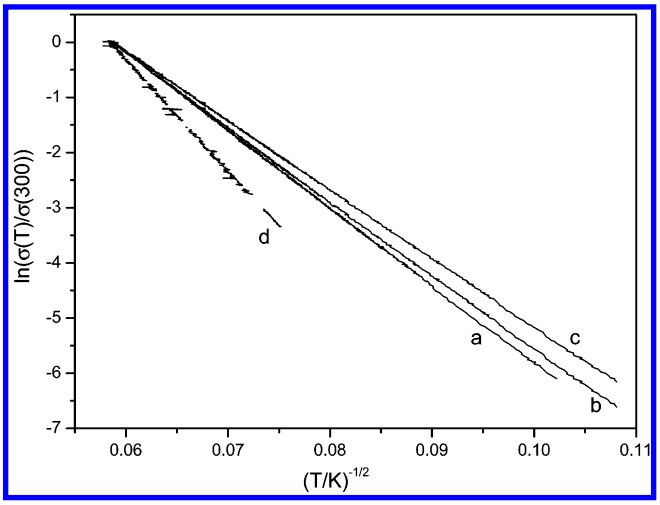

Figure 8. Temperature dependence of the conductivity of PANI−β-NSA (a) and PANI−β-NSA/TiO_2 with different contents of TiO_2, 0.04 M (b), 0.08 M (c), and 0.12 M (d). Synthetic conditions: [An] = 0.4 M, [An]:[β-NSA] = 1:0.5, [An]:[APS] = 1:1, reaction time 18 h, reaction temperature 0 °C.

The temperature dependence of the conductivity of the PANI−β-NSA/TiO_2 composite nanotubes prepared at different TiO_2 concentrations was measured from 300 to 77 K (see Figure 8). Some important results from Figure 8 can be summarized as follows. (1) The conductivity of all the samples decreases with decreasing temperature, showing a typical semiconductor behavior, which is similar to the results found for the conventional doped PANI. (2) The conductivity data of all the samples can best be expressed by the one-dimensional variable range hopping (1D-VRH) model,[43] by the following equation:

$$\sigma(T) = \sigma_0 \exp[-(T_0/T)^{1/2}]$$

where $T_0 = 8\alpha/(zN(E_F)k_B)$, in which α^{-1} is the localization length, $N(E_F)$ the density of states at the Fermi level, k_B the Boltzmann constant, and z the number of nearest neighbor chains. The T_0 value corresponding to the hopping energy barriers of charge carriers can be obtained from the slope of the straight line. (3) The T_0 value of granular PANI−β-NSA/TiO_2 was calculated to be 4.0×10^4 K, which was higher than that of the nanotubes (in the range of $(1.5-1.9) \times 10^4$ K). (4) Variation of the T_0 value with TiO_2 concentration is consistent with the change of its room-temperature conductivity.

As one knows, the water or oil contact angle can be used to characterize the hydrophilicity or hydrophobicity of materials.[44,45] Therefore, the water contact angle of PANI−β-NSA and PANI−β-NSA/TiO_2 films deposited on the glass substrate was measured. Typical photographs of a water drop on the PANI−β-NSA films are shown in Figure 9. The water contact angle of PANI−β-NSA nanotubes was measured to be ca. 53.5°, exhibiting hydrophilicity due to the hydrophilic $-SO_3H$ group of β-NSA. On the other hand, the water contact angle of PANI−β-NSA/TiO_2 nanotubes was enhanced with increasing concentration of TiO_2 (Figure 10), which may be due to the hydrophobic TiO_2 nanoparticles embedded in the wall of the nanotubes. These observations may open a route to change the hydrophilicity or hydrophobicity of PANI.

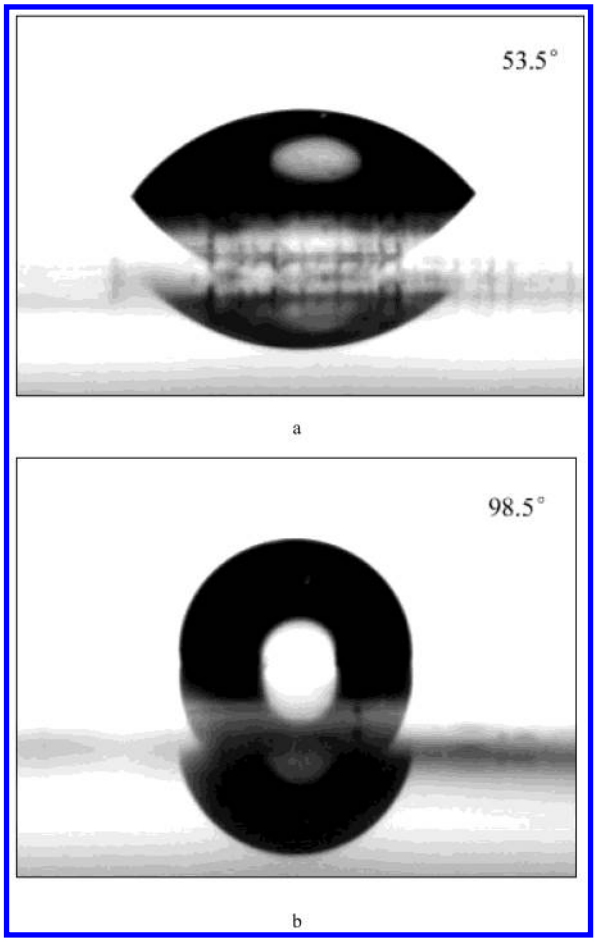

Figure 9. Photograph of a water drop on the PANI−β-NSA (a) and PANI−β-NSA/TiO_2 (b) films deposited on glass. Synthetic conditions: [An] = 0.4 M, [An]:[β-NSA] = 1:0.5, [An]:[APS] = 1:1, reaction time 18 h, reaction temperature 0 °C, (a) without TiO_2, (b) [TiO_2] = 0.08 M.

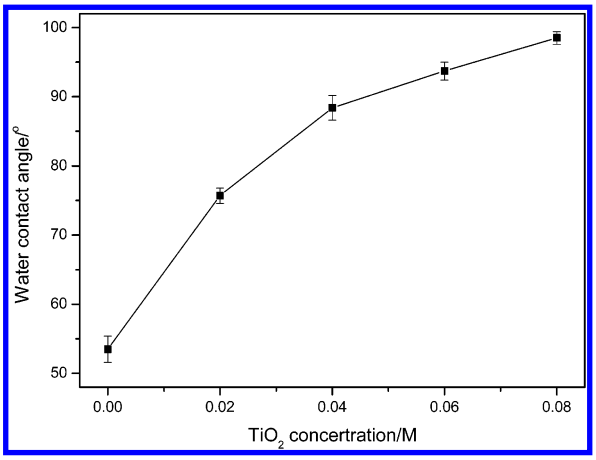

Figure 10. Effect of the concentration of TiO_2 on the water contact angle of the PANI−β-NSA/TiO_2 films deposited on glass. Synthetic conditions: [An] = 0.4 M, [An]:[β-NSA] = 1:0.5, [An]:[APS] = 1:1, reaction time 18 h, reaction temperature 0 °C.

Conclusion

We first demonstrated the possibility of PANI−β-NSA and TiO_2 nanoparticles costructuring to form PANI−β-NSA/TiO_2 composite nanotubes through a self-assembly process. It was found that the morphology, size, electrical properties, and hydrophobicity of the PANI−β-NSA/TiO_2 nanotubes were affected by the concentration of TiO_2. The core−shell micelles acting as templates, which consisted of aniline and β-NSA containing TiO_2 nanoparticles, were proposed to interpret the self-assembly formation of the PANI−β-NSA/TiO_2 nanotubes. Our employed method may be a simple and inexpensive route to synthesize or prepare multifunctional nanotubes of materials, which differs from that of coated or filled carbon nanotubes with other materials.

Acknowledgment. The National Natural Science Foundation of China (Grant No. 50133010) supported this project. TiO_2 nanoparticles were kindly supplied by Professor Jincai Zhao, Center for Molecular Sciences, Institute of Chemistry, Chinese Academy of Sciences. We also thank Professor Zhaojia Cheng and Mr. Yunzhe Long, Laboratory of Extreme Condition Physics, Institute of Physics, Chinese Academy of Sciences, for measuring the temperature dependence of conductivity.

References and Notes

(1) Chandrasekhar, P. *Conducting polymers, fundamentals and applications: a practical approach*; 1999.
(2) Kong, J.; Franklin, N. R.; Zhou, C.; Chapline, M. G.; Peng, S.; Cho, K.; Dai, H. *Science* **2000**, *287*, 622.
(3) Martin, C. R. *Science* **1994**, *266*, 1961.
(4) Huang, J.; Virji, S.; Weiller, B. H.; Kaner R. B. *J. Am. Chem. Soc.* **2003**, *125*, 315.
(5) Wu, C. G.; Bein, T. *Science* **1994**, *264*, 1757.
(6) Martin, C. R. *Chem. Mater.* **1996**, *8*, 1739.
(7) Michaelson, J. C.; McEvoy, A. J. *Chem. Commun*. **1994**, 79.
(8) Wei, Z.; Zhang, Z.; Wan, M. *Langmuir* **2002**, *18*, 917.
(9) Huang, L. M.; Wang, Z. B.; Wang, H. T.; Cheng, X. L.; Mitra, A.; Yan, Y. X.; *J. Mater. Chem.* **2002**, 12, 388.
(10) Yang, Y.; Wan, M. *J. Mater. Chem*. **2002**, *12*, 897.
(11) Huang, K.; Wan, M. *Chem. Mater*. **2002**, *14*, 3486.
(12) (a) Zhang, Z.; Wan, M. *Synth. Met.* **2003**, *132*, 205. (b) Tang, B. Z.; Geng, Y.; Lam, J. W. Y.; Li, B. Jing, X.; Wang, X.; Wang, F.; Pakhomovand, A. B.; Zhang, X. X. *Chem. Mater.* **1999**, *11*, 1581.
(13) Linsebigler, A. L.; Lu, G.; Yates, J. T. *Chem. Rev.* **1995**, *95*, 735.
(14) Luca, V.; Djajanti, S.; Howe, R. F. *J. Phys. Chem. B* **1998**, *102*, 10650.
(15) Lawton, L. A.; Robertson, P. K. J.; Cornish, B. J. P. A.; Jaspars, M. *Environ. Sci. Technol*. **1999**, *33*, 771.
(16) Matsumoto, T.; Murakami, Y.; Takasu, Y. *J. Phys. Chem. B* **2000**, *104*, 1916.
(17) Zubavichus, Y. V.; Slovokhotov, Yu. L.; Nazeeruddin, M. K.; Zakeeruddin, S. M.; Gratzel, M.; Shklover, V. *Chem. Mater.* **2002**, *14*, 3556.
(18) Somani, P. R.; Marimuthu, R.; Mulik, U. P.; Sainkar, S. R.; Amalnerkar, D. P. *Synth. Met.* **1999**, *106*, 45.
(19) Gurunathan, K.; Trivedi, D. C. *Mater. Lett*. **2000**, *45*, 262.
(20) Su, S.; Kuramoto, N. *Synth. Met*. **2000**, *114*, 147.
(21) Feng, W.; Sun, E.; Fujii, A.; Wu, H.; Niihara, K.; Yoshino, K *Bull. Chem. Soc. Jpn.* **2000**, *73*, 2627.
(22) Xia, H.; Wang, Q. *Chem. Mater*. **2002**, *14*, 2158.
(23) (a) Fan, J.; Wan, M.; Zhu, D.; Cheng, B.; Pan, Z.; Xie, S. *J. Appl. Polym. Sci*. **1999**, *74*, 2605. (b) Tang, B. Z.; Xu, H. *Macromolecules* **1999**, *32*, 2569. (c) Wei, Z.; Wan, M.; Lin, T.; Dai, L. *Adv. Mater.* **2003**, *15*, 136.
(24) Ajayan, P. M.; Iijima, S. *Nature* **1993**, *361*, 333.
(25) Wan, M.; Shen, Y.; Huang, J. J. Chin. Patent 98109916.5, 1998.
(26) Huang, J.; Wan, M. *J. Polym. Sci., Part A: Polym. Chem.* **1999**, *37*, 151.
(27) Wan, M.; Huang, J.; Shen, Y. *Synth. Met.* **1999**, *101*, 708.
(28) Wan, M.; Li, J. *J. Polym. Sci., Part A: Polym. Chem*. **2000**, *38*, 2359.
(29) Liu, J.; Wan, M. *J. Polym. Sci., Part A: Polym. Chem*. **2001**, *39*, 997.
(30) Hinrich, J.; Helfrich, W. *Chem. Rev.* **1993**, *93*, 1565.
(31) Kim, B. J.; Oh, S. G.; Han, M. G.; Im, S. S. *Langmuir* **2000**, *16*, 5841.
(32) Harada, M.; Adachi, M. *Adv. Mater*. **2000**, *12*, 839.
(33) Adachi, M.; Harada, T.; Harada, M. *Langmuir* **2000**, *16*, 2376.
(34) Quillard, S.; Louarn, G.; Lefrant, S.; MacDiarmid, A. G. *Phys. Rev. B* **1994**, *50*, 12496.

(35) Louarn, G.; Lapkoaski, M.; Quillard, S.; Pron, A.; Buisson, J. P.; Lefrant, S. *J. Phys. Chem.* **1996**, *100*, 6998.
(36) Bernard, M.; Goff, A. H. *Synth. Met*. **1997**, *85*, 1145.
(37) Cochet, M.; Louarn, G.; Quillard, S.; Buisson, J. P.; Lefrant, S. *J. Raman Spectrosc*. **2000**, *31*, 1041.
(38) Melendres, C. A.; Narayanasamy, A.; Maroni, V. A.; Siegel, R. W. *J. Mater. Res*. **1989**, *4*, 1246.
(39) Zhang, M.; Yin, Z.; Chen, Q. *Ferroelectrics* **1995**, *168*, 131.
(40) Tang, H.; Prasad, K.; Sanjinès, R.; Schmid, P. E.; Lévy, F. *J. Appl. Phys*. **1994**, *75*, 2042.
(41) Pouget, J. P.; Józefowicz, M. E.; Epstein, A. J.; Tang, X.; MacDiarmid, A. G. *Macromolecules* **1991**, *24*, 779.
(42) Cai, Z.; Lei, J.; Liang, W.; Menon, V.; Martin, C. R. *Chem. Mater*. **1991**, *3*, 960.
(43) Mott, N. F.; Davis, E. A. *Electronic Processes in Non-crystalline Materials*; Clarendon Press: Oxford, 1979.
(44) Carré, A.; Gastel, J. C.; Shanahan, M. E. R. *Nature* **1996**, *379*, 432.
(45) Onder, T.; Shibuichi, S.; Satoh, N.; Tsujiii, K. *Langmuir* **1996**, *12*, 2125.